Journal of Environmental Chemical Engineering 11 (2023) 109416

Contents lists available at ScienceDirect

Journal of Environmental Chemical Engineering

journal homepage: www.elsevier.com/locate/jece

Recent advances in photocatalysis on cement-based materials

Xiangyu Chen [a], Lige Qiao [b], Rixu Zhao [b], Jianhao Wu [a], Jingyang Gao [a], Lan Li [a], Jinchao Chen [a], Wen Wang [c], Melissa G. Galloni [d,e], Federico M. Scesa [f], Zhi Chen [a,*], Ermelinda Falletta [d,e,**]

[a] College of Materials and Chemistry, China Jiliang University, 258 Xueyuan Street, Xiasha Higher Education Zone, Hangzhou 310018, China
[b] China Construction Ready Mixed Concrete Co., Ltc., Wuhan 430070, China
[c] State Key Laboratory for Managing Biotic and Chemical Threats to the Quality and Safety of Agro-products, MOA Laboratory of Quality & Safety Risk Assessment for Agro-products (Hangzhou), Institute of Agro-product Safety and Nutrition, Zhejiang Academy of Agricultural Sciences, Hangzhou 310021, China
[d] Department of Chemistry, University of Milan, via C. Golgi, 19, Milan 20133, Italy
[e] Consorzio Interuniversitario Nazionale per la Scienza e Tecnologia dei Materiali (INSTM), via Giusti 9, Florence 50121, Italy
[f] Department of Chemistry Materials and Chemical Engineering (DCMC), Polytechnic of Milan, Piazza Leonardo da Vinci, 32, Milan 20133, Italy

ARTICLE INFO

Editor: Dr. G. Palmisano

Keywords:
Visible-light photocatalysis
Cement-based photocatalytic materials
Multifunctional materials
NO_x degradation
Organic pollutant degradation
Preparation and Photocatalytic Mechanisms

ABSTRACT

Cement is a crucial material for modern infrastructure and is mainly used as a structural material worldwide. Recently, the development of cementitious materials with accessional functionality for further expanding the applications has been rapidly growing. Cement with photocatalytic functions has dual functionality of construction and the photodegradation of pollutants. This topic has drawn rapidly-growing interest around the world, and progress has been achieved in the preparation and applications. However, a comprehensive overview of the recent advances is still absent. Herein, we summarize the recent advances in cement-based photocatalytic materials, mainly focusing on their preparation and performance. Examples of practical applications are also given, and the challenges and strategies for multifunctional cements with photocatalytic properties are provided at the end. This review may benefit the design of novel cement-based materials with multifunctions for further applications.

1. Introduction

Cement is the key material in meeting the essential needs of the current global housing and modern infrastructure with a long history. According to the archaeological findings [1], a mixture of ground stone and loess was found at the site of the Yangshao culture about 5000–3000 years ago. In ancient Europe, Roman mortar made from lime, volcanic ash, and sand could be regarded as the predecessor of modern cement. The consumption of cement is positively correlated with the growth of world GDP (Gross Domestic Product) [2]. With the continuous maturation of cement manufacturing technology [3], modern cement has reached high compressive strength [4], and good plasticity before setting. Moreover, it has good serviceability and can maintain its performance in long-term hot and cold cycles as well as wet and dry cycles. Therefore, according to Fig. 1**(a)** (IEA Cement roadmap targets, 2009) [5], the demand for cement in industrial production and social life is continuously growing.

Cement production is expected to grow significantly between 2020 and 2050. With this significant increase in cement production, several issues (i.e., rising energy demand, CO_2 reduction requirements, and raw material availability) need to be seriously considered. The calcination process in cement production (formation of CaO from $CaCO_3$ decomposition) releases large amounts of CO_2, contributing to the global warming resulting in growing concern worldwide. Currently, the atmospheric CO_2 levels are close to 380 ppm [6], and this is a serious threat to global survival and sustainability. However, to date there are no effective techniques and policies to change this situation, and CO_2 concentrations may increase to more than 800 ppm by the end of the century [7]. However, the use of alternative fuels to reduce CO_2 levels has rapidly increased in recent years and will be expanded in the future [8–10].

In the cement industry, the clinker factor reduction [11,12] is a key priority, and intensive efforts have been devoted to improving cement technology. Although innovative materials have been developed, the extent to which they can replace the current cement-based materials remains to be seen [5]. Cementitious materials are internally filled with

* Corresponding author.
** Corresponding author at: Department of Chemistry, University of Milan, via C. Golgi, 19, Milan 20133, Italy.
E-mail addresses: zchen@cjlu.edu.cn (Z. Chen), ermelinda.falletta@unimi.it (E. Falletta).

https://doi.org/10.1016/j.jece.2023.109416
Received 12 December 2022; Received in revised form 25 January 2023; Accepted 31 January 2023
Available online 1 February 2023

capillary-like voids and possess abundant porous spaces. Therefore, water infiltration occurs in the cement structure due to rainfall and other unfavorable weather conditions over time [13]. Long-term lasting water infiltration accelerates the destruction of the internal structure of cementitious materials and, meanwhile, could lead to the infestation of the surfaces with bacteria, fungi, and insects, making the porous structure inside the cement a breeding ground for these species. Microorganisms' spread not only results in environmental pollution, but also leads to serious human health diseases, like cough and asthma. Modifying cementitious materials with proper photocatalysts may make cement composite highly bactericidal, eliminating the hazards caused by moisture. Furthermore, to solve these problems [14], the functionality can be enhanced by combining cement with proper compounds. The interaction among different materials improves the strength, weight, stiffness, fatigue, toughness, ductility, crack resistance, and other matrix properties. We, therefore, refer to cement with photocatalytic functions as cement-based photocatalytic materials. The development of environmentally friendly multifunctional photocatalytic cements is promising in the cement market [15–17], enriching the cement functionality by adding or coating materials with hydrophobic or antimicrobial and photocatalytic properties [18]. In this regard. academic research has gained growing attention and the related publications increase annually, as shown in Fig. 1**(b)**. However, an overall and timely summary is still missing.

This work presents a comprehensive review of the recent advances in the fabrication and application of multifunctional photocatalytic cement in the degradation of air pollutants. Firstly, the different strategies for composites' preparation are summarized, classified and critically discussed. Then, the mechanical and catalytic properties of the obtained materials are investigated. Meanwhile, examples of the application of cement-based photocatalytic materials for environmental remediation in several countries are given. Finally, problems and challenges are overviewed and discussed.

2. Characteristics of photocatalytic materials and their applications

According to the World Health Organization (WHO) [19,20], air pollution is defined as the contamination of outdoor or indoor air by organic and inorganic chemical pollutants. Currently, the most common methods for removing air pollutants are filtration and adsorption [21]. However, these methods deal with physical removal, and therefore require to replace, clean, and reprocess the active materials after pollutants' absorption, producing a potential drawback. In contrast, UV radiation and ozone disinfection are alternative technologies to kill harmful germs as well as organic contaminants. However, they have adverse effects on human health, or require additional energy source. Therefore, it is urgent to develop an effective, safe, and inexpensive technology to break down as many air pollutants as possible. In this context, photocatalytic technology is one of the most promising methods for air purification.

2.1. Photocatalytic mechanism

The electronic energy band of semiconductor photocatalysts consists of an electron-filled valence band (VB) and a vacant conduction band (CB) separated by a bandgap (Eg), acting as the energy barrier for the electron transition [22]. As shown in Fig. 2, when the semiconductor absorbs energy from photons of sufficient energy, electrons in the VB can be excited to the CB through the energy barrier, leaving an equal number of holes in the VB. The photoproduced charges can diffuse to the photocatalyst surface to take part in the redox reaction [23,24].

The migrated electrons and holes have strong reactivity and can react with substances adsorbed on the surface of the semiconductor or dispersed in solution. By way of example, the holes can oxidize electrons donors into hydroxyl radicals (e.g., OH^- into ·OH), whereas the photogenerated electrons can reduce electron acceptors (e.g., O_2 dissolved in an aqueous solution or present in the air to form hydrogen peroxide or superoxide anion radicals,$\cdot O_2^-$ respectively). The formed reactive species have strong redox ability exploitable for several applications, including H_2 production, disinfection, CO_2 reduction, wastewater treatment, and air purification.

However, alternatively the photogenerated charges can undergo recombination processes both in the bulk or at the surface effectively nullifying their reactive properties.

The ability of the photogenerated charges to carry out redox reactions is strictly related to the relative redox potential of the electronic band structure and to those of both electron donors and acceptors. More in detail, for the reduction reaction to take place, the CB energy level has to be more negative than the redox potential of the involved electron acceptor. Conversely, the oxidation reaction only occurs if the energy level of the VB is more positive than the involved electron donor.

Another important consideration is the lifetime of the charge carriers versus the recombination rate. In fact, the performance of each photocatalyst is related to the ability of the free charges to reach the surface and carry out redox reactions with the adsorbed species or detach from the surface producing reactive oxygen species (ROS), typically •OH, $\bullet O^{-2}$, $HO_2\bullet$, and H_2O_2. These latter can further react to form other ROS. These highly active species are able to decompose organic and inorganic pollutants into CO_2, H_2O, N_2 H_2CO_3, HNO_3, and H_2SO_4.

Photocatalysts may be roughly divided into several types based on their compositions: oxygen-free photocatalysts and metal oxide-based photocatalysts.

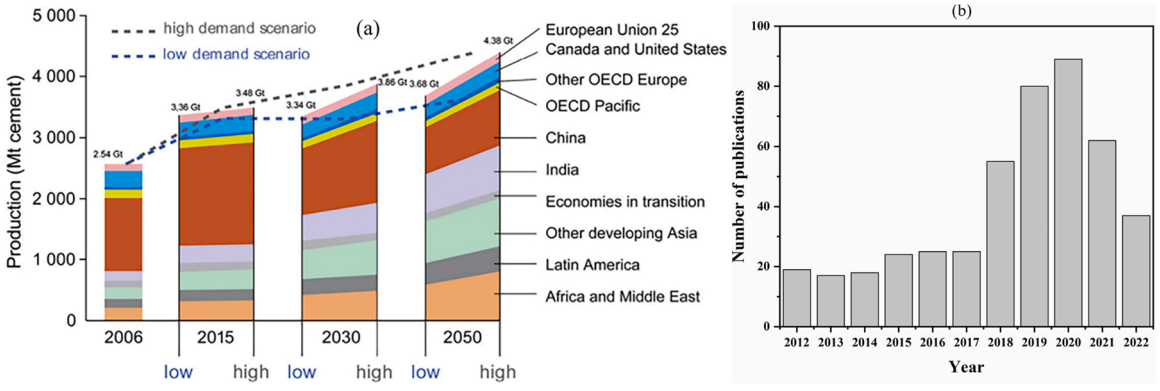

Fig. 1. (a) Global cement production [5] and (b) Number of recent publications on photocatalysis technology in cement research searched by the keywords "cement" and "photocatalysis" (collected from Web of Science core database. November 19, 2022).

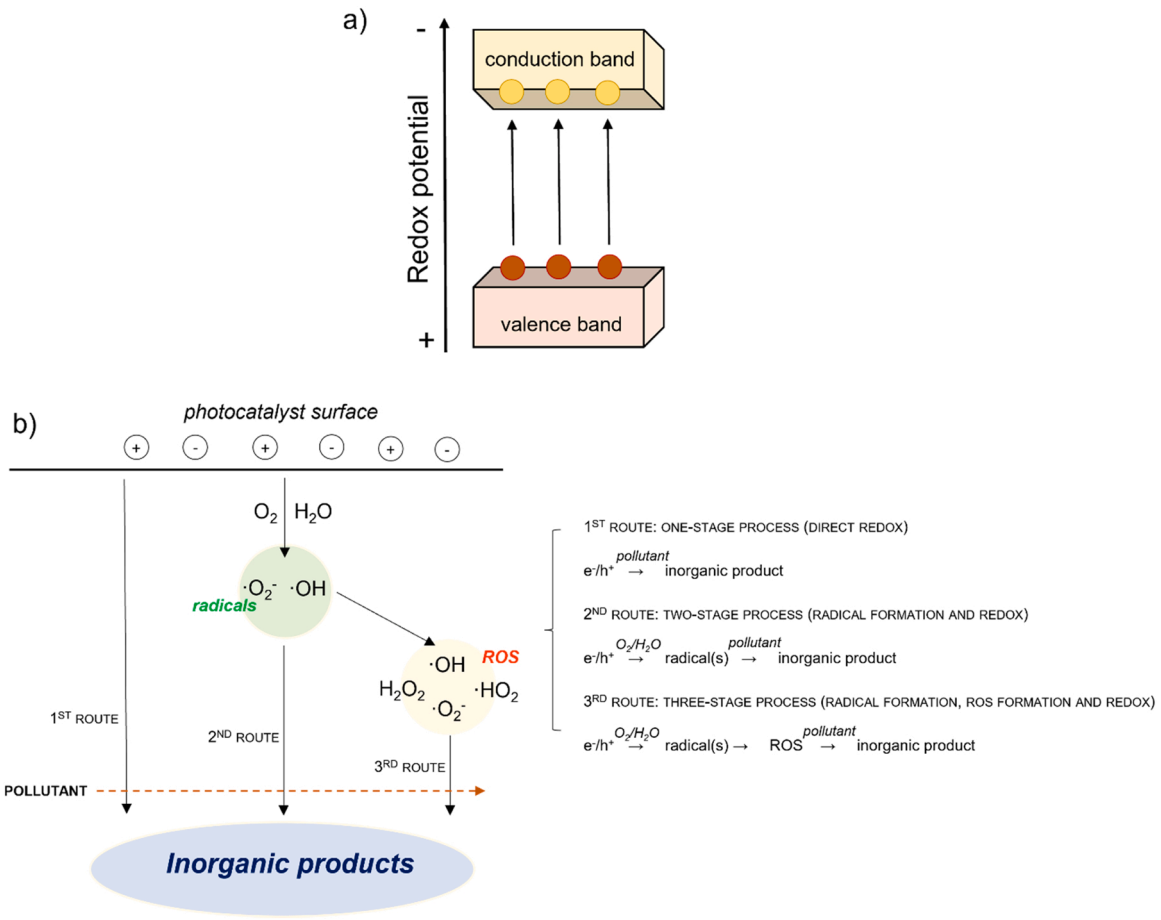

Fig. 2. Schemes of electron and hole transfer (a) and of three possible mechanisms of photocatalytic degradation of pollutants (b).

2.2. Oxygen-free photocatalysts

Many oxygen-free compounds have shown interesting photocatalytic properties. Among them, some metal sulfides, including molybdenum sulfide (MoS_2), tungsten sulfide (WS_2), copper sulfide (Cu_xS_y), zinc sulfide (ZnS), and cadmium sulfide (CdS), are interesting thanks to their special structures and excellent physicochemical properties. In addition to sulfides, in recent years the most promising application has been found on graphite-phase carbon nitride (g-C_3N_4). Both CdS and g-C_3N_4 have shown wide applications in photocatalysis [25]. Since the discovery of g-C_3N_4, an n-type metal-free polymer semiconductor, for photocatalytic hydrogen production [26], related research in photocatalysis has rapidly grown and has become a hot topic. Compared to conventional semiconductors (e.g., TiO_2 and ZnO) g-C_3N_4 with two-dimensional (2D) layered structure and π-conjugated system (Fig. 3) has a more suitable bandwidth (~2.7 eV) [27], conferring good photocatalytic performance. The graphite-like lamellar structure of g-C_3N_4 is composed of three homogeneous units connected by N-atomic triangular cross-linking in the plane, exhibiting a stable structure with good thermal and chemical stability.

Although the pristine g-C_3N_4 demonstrates great potential in H_2 production [28,29] and pollutant degradation [30,31], its photocatalytic efficiency remains low due to the rapid recombination of the photogenerated charges. The improvement of morphology, such as exfoliation of g-C_3N_4 into g-C_3N_4 nanosheets (g-C_3N_4, 2–3 nm thickness), is an effective way to improve its photocatalytic performance [32,33].

Recently, great strides have been made in modifying g-C_3N_4-based materials to increase their performance. Lu et al. demonstrated the enhanced photocatalytic activity in the field of both pollutants' degradation and hydrogen production of novel Z-scheme g-C_3N_4/Ag/MoS_2 ternary heterojunctions consisting of flowerlike superstructures [34], whereas Tatykayev and coworkers reached faced the topic by the use of g-C_3N_4/TiO_2 composited obtained by thermolysis of MIL-125(Ti) in the presence of g-C_3N_4 decorated with NiS nanoparticles [35]. Moreover, Z-scheme g-C_3N_4/$Bi_4Ti_3O_{12}$/$Bi_4O_5I_2$ heterojunctions exhibited surprising activity in the simultaneous hydrogen production and photocatalytic degradation of antibiotics [36].

CdS is a semiconductor with 2.42 eV bandwidth (Fig. 4) that makes it efficient in visible light photocatalysis [37,38]. More importantly, the conduction band position of CdS is lower than that of other common semiconductors, such as TiO_2, $SrTiO_3$, and ZnO [39]. This means that the photoelectrons from CdS have a stronger reduction ability in photocatalytic reactions, extensively exploited in visible-light-induced photocatalysis, as well as in other sectors. In addition, CdS is prone to photo-corrosion and would decompose into sulfur monomers and cadmium ions that cause the loss of catalytic activity. The photo-corrosion severely retards the photocatalyst recycle, hindering its practical application. To solve this crucial problem, the most common approach is to combine CdS with other semiconductors with suitable band gaps to prevent the rapid onset of photocorrosion phenomena, and thus to extend the catalyst lifetime [40,41]. Nowadays, CdS-based photocatalysts have been widely used in photocatalytic disinfection, H_2 production, CO_2 reduction, wastewater treatment, and air purification.

2.3. Metal oxide-based photocatalysts

TiO_2 has been the most investigated photocatalyst since Fujishima and Honda's pioneering work on photocatalytic water splitting in 1972 [42]. Due to the high activity, stable performance, low cost, and

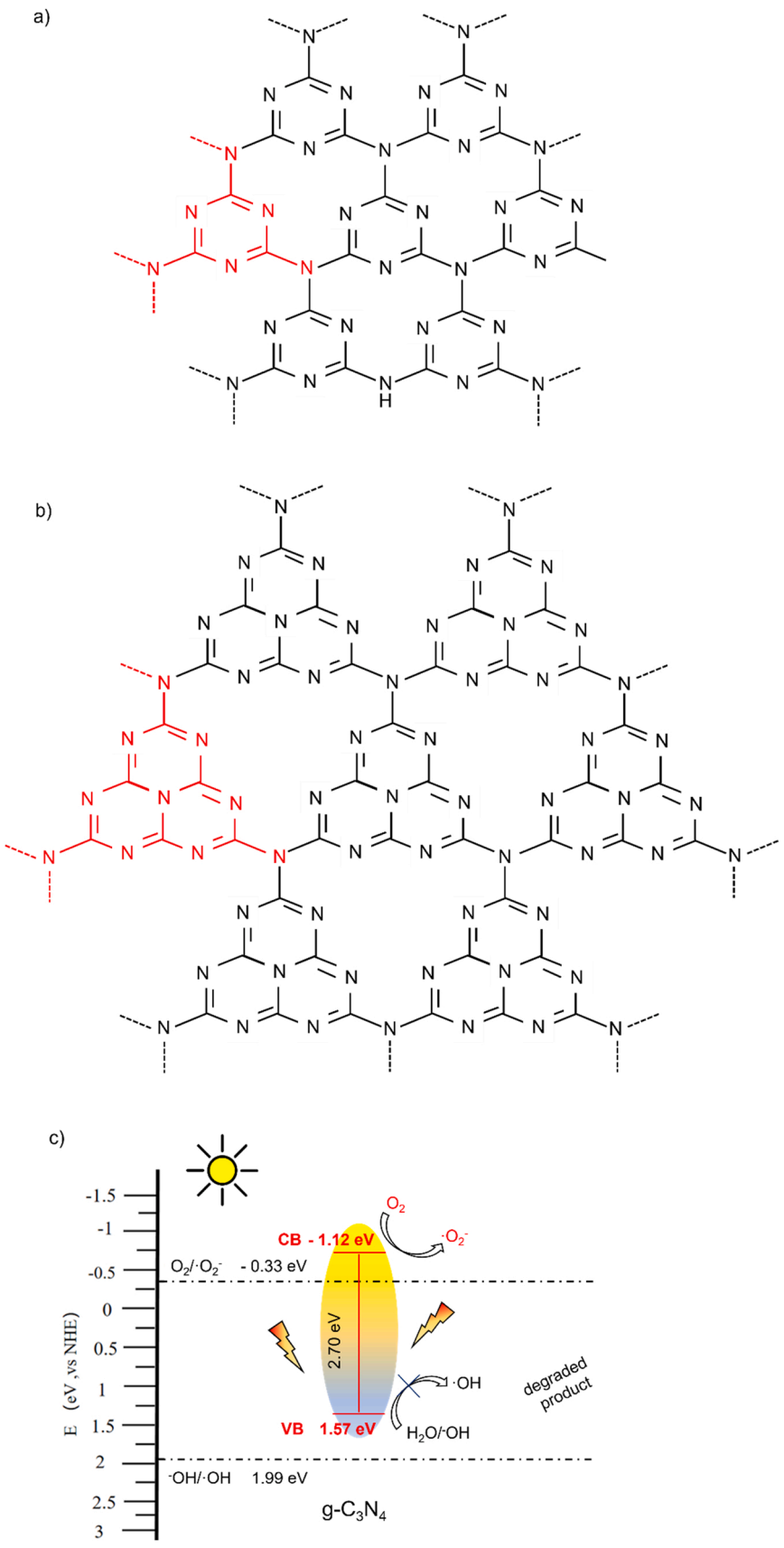

Fig. 3. g-C_3N_4: triazine and tri-s-triazine structures (a, b) and photocatalytic mechanism (c).

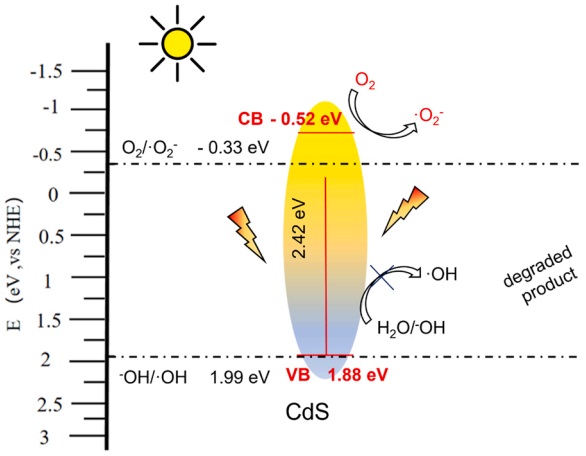

Fig. 4. Photocatalytic mechanism of cadmium sulfide.

non-toxicity, TiO_2-based photocatalysts have been widely used for air purification, water pollutants' degradation, antibacterial disinfection, deodorization, and anti-fogging. However, TiO_2 has two major drawbacks: one is its wide band gap (3.0–3.2 eV) that leads to poor visible-light utilization, and the other relates to the high recombination of the photogenerated electron-hole pairs, resulting in low quantum efficiency [43]. To solve this problem, modifications on TiO_2 have been done to improve the utilization of visible light and reduce the photogenerated electron-hole recombination rate on the TiO_2 surface. Diverse strategies, including photosensitization of semiconductor surfaces, deposition of noble metals on semiconductor surfaces, metal/non-metal doping, and modification with other semiconductors, have been reported to improve its photocatalytic efficiency [42,44].

Bismuth-based oxides are an alternative category of photocatalysts with wide applications [45–47]. Among them, Bi_2O_3 has unique properties, such as high electrical conductivity and a narrow bandgap (~2.8 eV) that make it interesting for applications under visible light or solar light irradiation [48,49].

Bismuth-based semiconductor materials have substantially alleviated the problem of poor visible-light adsorption due to their suitable band gap (Fig. 5) [50]. However, the low quantum efficiency and the high photogenerated carrier recombination rates remain the key issues to be addressed for bismuth-based photocatalysts.

In this regard, important advances have been done. For example, the addition of silver halides, in particular AgBr, permits the fabrication of AgBr/BiOBr heterojunctions able to improve the utilization of sunlight, charge separation efficiency and redox ability of BiOBr [51–53]. Advantages and feasibility of cement-based photocatalytic materials.

When applying the photocatalysts to the practical degradation of pollutants, one main concern needs to be considered: a proper support is required to load the photocatalyst for high activity and long-term durability.

Cement-based materials loaded with powerful photocatalysts may be good candidates for treating urban air pollutants because they are the most used materials in modern buildings. For example, multifunctional urban building walls may simultaneously absorb and degrade outdoor air pollutants, as well as degrade indoor pollutants, such as formaldehyde [54]. Airborne nitrogen oxides ($NO+NO_2$), generally identified as NO_x, are one of the most common sources of external pollutants [55–57]. NO_x contribute to the formation of photochemical smog that is related to lung problems and asthma in humans [58]. Composites containing photocatalysts have demonstrated great potential to reduce NO_x concentrations [59,60]. Hardened cement pastes possess a porous structure with a strong binding capacity that is well suited for immobilizing photocatalyst powders and other photo-oxidation products. Many laboratory studies and pilot projects have demonstrated that concrete pavements and exterior building surfaces are the best media for loading photocatalyst [61] because the flat structure of the pavement can directly expose the photocatalyst to sunlight and airborne contaminants. This is particularly significant for the places with high-level pollution, such as high-traffic canyon streets, highway tunnels, and urban environments. Generally, the most common photocatalyst employed, TiO_2, is immobilized on the top layer of the concrete pavement for best performance, and the reaction products adsorbed on the surface can be washed away by rainwater. Moreover, nanosized photocatalysts may be used as architectural coatings in civil engineering. The addition of nanosized photocatalysts to architectural coatings can greatly improve the basic properties of traditional coatings, such as enhanced mechanical strength, adhesion, water resistance, and stain resistance. Moreover, it may endow architectural coatings with multi-functions of purifying harmful pollutants in the air. However, abrasion and other phenomena can lead to the photocatalysts detachment from the concrete surface. For this reason, other strategies have been developed to incorporate photoactive particles in cementitious materials, as described below.

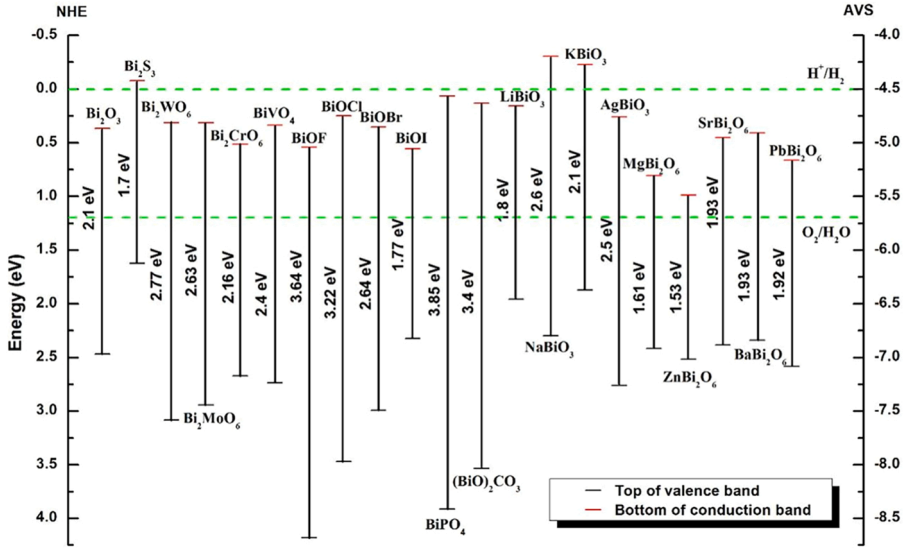

Fig. 5. The energy band position of bismuth-based photocatalysts [50].

3. Preparation method of cement-based photocatalytic materials

The incorporation of photocatalytic particles in concrete is still a challenge. Here, the main goal is the introduction of the maximum amount of catalyst at the material surface, avoiding losing it for phenomena as abrasion or weathering. In this context, two main methods have been developed: mixing photocatalytic particles with cementitious materials (mechanical mixing), and coating the concrete surface with formulations containing photocatalysts (coating).

3.1. Mechanical mixing

It consists in the embedding of photoactive particles in the cementitious materials. The main advantage of this approach consists in improving the protection of the photocatalyst from harsh and aggressive environment. However, it is evident that by the mixing method the catalyst cannot be uniformly dispersed in the cement, producing an effect on the strength of the formed cement. In addition, this approach does not allow a majority distribution of the particles on the cement surface. Indeed, only a small percentage will occupy the surface layer, whereas the rest will remain incorporated in the bulk, strongly reducing the direct contact between the catalysts and the contaminants, thus leading to a reduction in photocatalytic efficiency.

The mechanical stirring and dispersing method need strong centrifugal force, pressure, and shear force generated by mechanical motion to uniformly disperse the agglomerated catalyst particles in the liquid medium. The continuous addition of water during the stirring can promote the catalyst particles' dispersion. He et al. [62] prepared cement-based photocatalyst composites by stirring the photocatalyst with cement slurry. The planetary high energy ball milling method was employed for the modification of nano-TiO_2 to obtain Fe^{3+}-doped nano-TiO_2. It was observed that the Fe^{3+} modification caused significant changes to the nano-TiO_2 characteristics, such as particle size reduction, increase of amorphous morphology, etc. The photocatalysts and cement powders were firstly mixed under dry conditions, and then water was slowly added and continuously stirred to form the cubic specimen blocks. After curing for 24 h, the cube specimen was removed from the mold and placed in a standard curing chamber and cured in a temperature and humidity environment under standard conditions for 28 days to obtain the final product. The investigation demonstrated that the nano-TiO_2 incorporation improved the concrete strength thanks to the micro-filling effect of the nanomaterials. In addition, concerning the doped-photocatalysts the presence of Fe^{3+} sites permit the formation of hydration products, leading to a further increase of concrete strength. In general, Fe^{3+}-doped nano-TiO_2 exhibited higher photocatalytic performance than the pristine nano-TiO_2. However, both materials permitted to achieve interesting results when introduced in the cement at a percentage of 3 or 4%. Chen et al. [61] prepared cement-based photocatalytic materials with different proportions of the components according to the following processes. The water/cement ratio was maintained at 0.35, whereas the amount of photocatalyst added was 5% or 10% of the total weight of cement. A smooth, well-mixed slurry was first produced by mechanical stirring. Then, it was poured into a laboratory-made mold. Molds were vibrated by a shaker to allow further dispersion of the catalyst within, thus ensuring that the cement slurry is thoroughly compacted internally. The finished sample is then cured in an environmental chamber for 24 h. The results demonstrated that the key factors responsible for the photocatalytic activity were the surface area of the catalyst and the presence of metallic contaminants in the final composite. These latter may absorb or block part of the incident photons necessary for the photocatalytic reaction and at the same time could contribute to the electron-hole recombination, deactivating the photocatalyst. Eventually, an important role is also attributed to the curing age, related to the cement hydration products that filling up capillary pores are able to create diffusion barriers to both reactants and photons. Singh et al. [18] used a mortar to mix and grind cement with the prepared catalyst and dried it to obtain the target photocatalytic material. During the mixing process, a small amount of water was added to the mixture to accelerate the catalyst dispersion to form a smooth paste-like composite, and the paste was transferred into a cylindrical casting mold immediately after completing the mixing to dry and obtain the final product. In this regard, Janus et al. [63] investigated the effect of nitrogen-modified TiO_2 (N-TiO_2) as photoactive additive added in the percentage of 1, 3, and 5 wt% to the total weight of cement, chosen for the possibility of being produced in the amount of 0.5 kg *per* day. The best results in terms of photocatalytic capacity, stability of the mechanical properties of the cement, increase of the compressive and the flexural strength were obtained with 5 wt% N-TiO_2 loaded into the cement mortar. Singh et al. [18] investigated the enhanced photocatalytic, hydrophobic and antimicrobial properties of concrete when modified with ZnO additive (5–15%), demonstrating that the effect is dose-dependent and reaching the best results for high ZnO loads. Lu et al. [64] first mixed the cement powder with Na_2SO_4 to prepare a cement-based foam photocatalyst with uniform pore size. Then, water and hydrogen peroxide were gradually added to the mixture. The TiO_2 particles were slowly dispersed into the fresh mixture, and the final composite was molded into cubes for evaluating the photocatalytic activity. The surface open pores enhance the porosity of foam cement allowing the UV light to deeply penetrate inside the cement matrix activating TiO_2 particles for the photocatalytic process. Foam cement with 0.3 wt% TiO_2 exhibited the highest photodegradation performance Differently, Geng et al. [65] investigated the photodegradation of rhodamine B and nitrogen oxides on cement-based materials doped with BiOBr. The bismuth-based composites were prepared by firstly mixing and placing the cement powder in pure water with another suspension containing BiOBr with a mechanical stirrer following a drying and molding process. The advantage is that the preparation process is simple, the water/cement ratio is adjustable (1800/630 g/g, 1800/380 g/g) as well as the autoclave curing time (0–6 h), and the catalyst is relatively uniformly dispersed in the cement by mechanical mixing. It was demonstrated that by the use of the BiOBr-modified concretes the photocatalytic performance increased with the extension of autoclaved curing time even if not proportionally. The materials characterized by higher porosity promoted better photocatalytic activities. Concerning the photodegradation processes under visible light irradiation, the best results were obtained with modified cements produced by a water/cement ratio 1800/630 g/g at each autoclaved curing time. In fact, these composites permit an ease passage of the light through the pores.

3.2. Dispersants

As catalysts are mostly micron- or nano-sized particles with a large specific surface area and high surface energy, they can easily clump together, reducing the exposure of the active site to air pollutants. Therefore, high efficiency can be only achieved with the adequate dispersion of the catalyst. The addition of proper dispersants can enhance the catalyst particles dispersion by different mechanisms. Anions present in water may be adsorbed on the surface of the catalyst particles by adding appropriate electrolytes (sodium tripolyphosphate, sodium silicate, and sodium sulfate) to the solution, or by adjusting the pH to prevent them from aggregation due to their repulsive forces [66, 67].

3.3. Ultrasonic dispersion

Ultrasounds are characterized by short wavelengths and concentrated energy. Under ultrasounds the microbubbles rapidly nucleate in the medium, exploding when the pressure reaches critical conditions, producing a local huge shock wave and high-speed airflow to promote high particle dispersion [68,69]. This method is generally used as an alternative, or an auxiliary means of mechanical stirring to accelerate the dispersion of catalysts in concrete [70].

3.4. Coating

By this approach, the photocatalyst is prepared as a colloid or suspension and then coated on the concrete surface to endow the surface photocatalytic properties. The catalyst coating on the concrete surface has little effect on noumenal mechanical properties. The durability and wear resistance of the coating may have the main impacts on the final performance. By the mixing approach Hassan et al. [71] applied a mixture of catalyst and cement to the surface of a pre-formed cement to obtain a 10 mm thick photocatalyst-cement coating to evaluate the environmental performance of TiO_2 particles before and after laboratory-simulated abrasion and wearing. The cement loaded with 5% TiO_2 showed the best efficiency in NO degradation. However, after the wear test it resulted in a small reduction of NO removal ability. On the contrary, in the same conditions 3% TiO_2 loaded cement enhanced a little bit its performance. Since EDS analyses did not evidence differences on the two samples, a more in-depth study is needed to understand the reasons that cause the different behavior of the two materials. Feng et al.[72] and Wang et al. [73] sprayed a catalyst suspension on the cement slurry surface to form a liquid layer that was dried to obtain a properly photocatalytic composite material. Feng and his coworkers achieved the best photocatalytic performance, uniform particles distribution, high stability and good mechanical strengths by the use of 10 wt % TiO_2 content in suspension and three spraying times [72]. Wang's investigations were oriented towards the replacement of TiO_2 particles with visible active BiOBr@SiO_2 flower-like nanospheres [73]. The results showed that the photocatalytic activity of the materials was two times higher compared with the traditional TiO_2-modified cement sample. Moreover, based on the IARC study of March 2020, TiO_2 is classified as "possibly carcinogenic to humans" (group 2B) [74,75]. Therefore, as an alternative Peng et al. [76] prepared advanced muscovite sheet/SnO_2/g-C_3N_4 coatings. The fabrication of muscovite sheets into photocatalytic cement permits to reduce the photogenerated carriers' recombination and, moreover, prevents the carbonation of cement due to products of the photocatalytic reaction. The authors demonstrated that the photocatalytic performance of the material is strictly related to the amount of muscovite sheet/SnO_2 (MS) powder employed. In fact, the best mechanical and photocatalytic properties of cement were obtained when the photoactive coating was prepared by the use of 0.6 g MS powder and 20 g urea (g-C_3N_4 precursor). The main advantage of the coating method is that the process is simple and relatively feasible for large-scale applications. However, the photocatalyst is attached to the cement surface as a coating via this method, and the cement only provides a carrier for the photocatalyst, not protection. Therefore, it is necessary to improve the adhesion of the photocatalyst coating to ensure long-term photocatalytic capacity against external mechanical forces and natural environments.

4. Characterization

4.1. Mechanical properties

Due to their porous nature, cement-based materials have a strong adsorption ability. The use of cementitious materials as carriers for loading photocatalysts not only makes full use of the special porous structure of concrete, but also has a certain impact on its mechanical and compressive properties. According to the mechanical tests on photocatalytic cement-based materials carried out by He et al. [62], the compressive strength of the concrete first increases and then decreases increasing the TiO_2 content. The results show that the incorporation of TiO_2 nanoparticles could enhance the concrete strength, which is mainly due to the micro-filling effect of TiO_2, making the internal structure of concrete denser and thus leading to enhanced strength. The increase in maximum strength was about 5%. However, when the nanomaterial content exceeded a certain range, the strength of the composite decreased, probably due to the catalytic particles' agglomeration, which leads to a non-uniform distribution of these latter in the structure, causing some decrease in the concrete strength. Lee et al. [77] showed that nano-TiO_2 can significantly promote the cement hydration and improve the compressive strength of cement mortar. The incorporation of catalyst particles into cement can improve the filling effect. Moreover, the catalyst particles can be used to change the hydration environment through the size effect, enhancing the microstructure of the hardened cement paste and jointly strengthens the physical properties of the cementitious material. Based on this advantage, nano-TiO_2 can be added to an unformed cement slurry to produce hydration products rapidly. The addition of TiO_2 in the hydration process of cement makes the photocatalytic nanoparticles the "core", further accelerating the accumulation of hydration products and contributing to the improvement of the physical properties of cement products. At the same time, nano-TiO_2 distributed in the slurry will act as network nodes between the hydration products. Based on the original network structure of the cement-hardened slurry, a new network with nanoparticles as network nodes is established, combining more nanoscale C-S-H bonds (calcium silicate hydrated minerals) to form a dense three-dimensional network structure [78]. The strength of cement mortar is closely related to the content of C-S-H bonds in the gels. Wang et al. and Jafari et al. used SiO_2 with BiOBr as the active photocatalyst, resulting in a significantly lower pore content in concrete than in untreated concrete. This may be due to the formation of a large amount of gel on the surface of the treated white cement paste, making it denser and smoother. Based on the reaction between BiOBr@SiO_2 and $Ca(OH)_2$, the presence of SiO_2 can induce the formation of C-S-H gel [73] that enhances the immobilization of photocatalysts on the concrete surface. Janus et al. [68] determined the compressive and flexural strength of pure cement and cement mixed with 1, 3, and 5 wt% of N-TiO_2. As shown in Fig. 6**A**, the compressive strength of the unmodified cement reached 53 MPa (red line), whereas all the modified materials demonstrated improved compressive strength. The highest compressive strength (57.4 MPa) was achieved by the composite at 1 wt% of N-TiO_2, whereas the minimum increase in compressive strength was observed with 5 wt% of N-TiO_2. Similar performances were observed in the flexural strength tests, as shown in Fig. 6**B**. These results demonstrate that the mechanical properties of the cement (compressive and flexural strength) were significantly influenced by the level of N-TiO_2 doping. However, He et al. found that the distribution inhomogeneity problem became severe as the nanoparticles content increased. Densely distributed nanoparticles cause agglomeration phenomena, forming many clusters, resulting in an inhomogeneous microstructure. This leads to a decrease in the strength of the cement as the nanocatalyst content rises [62].

Dense irregular network crystals inside the cement mortar may be formed as the age increases due to the hydrophilicity of nanosized TiO_2 (as shown in Fig. 7), avoiding the cracks. Zhang et al. [79] found that the degree of cement hydration decreased with the increasing nano-TiO_2 content, probably for the small size and large surface area of nano-TiO_2, which requires more water absorption, resulting in a decrease in the degree of the cement hydration. Ma et al. [80] analyzed the internal porosity of the hydrated 28 days mortar doped with nano TiO_2 by the MIP method (Mercury Pressing Method) and revealed that the porosity was minimized at 3% nanosized TiO_2 doping. Feng et al. [81] discovered that the flexural and compressive strength of cement stone modified with 0.9% nanosized TiO_2 increased by 16.12% and 14.15% at 28 days, respectively. Perdikatsis et al. [82] reported that the compressive strength of cement mortar containing 3% nano-TiO_2 at 28 days of age was 38.86% that is lower than that of the reference group. On one hand, the modulus of elasticity and flexural strength increased by 40.48% and 5.21%, respectively, whereas the compressive strength at three weeks and one year of age increased by 21.7% and 45%, respectively. Feng et al. [81] observed that after 28 days of making the composites the flexural strength of the cement coated with the catalyst layer was significantly increased compared to the pure cement due to the formation of a waterproof layer on the surface of the coating catalyst.

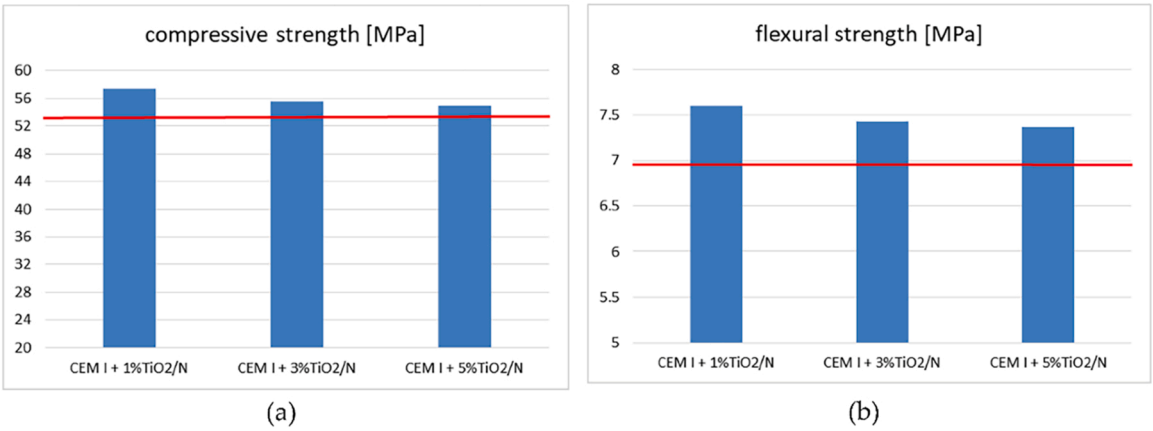

Fig. 6. (a) Compressive and (b) flexural strength of 1, 3, and 5 wt% of photocatalyst N-TiO_2. In the red line, the compressive strength (53 MPa) and flexural strength (6.92 MPa) of unmodified cement were presented [63].

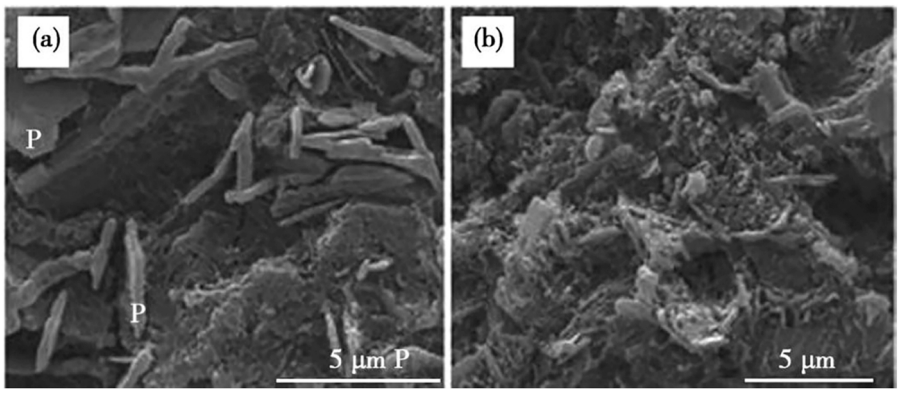

Fig. 7. Hydration of lime-metakaolin specimens: (a) without nano-TiO_2, P as silicate crystals; (b) with nano-TiO_2 [83].

However, the addition of the TiO_2/waterproof layer did not have a significant effect on the compressive strength of the mortar. As an alternative, Geng et al. [65] used BiOBr, revealing that the compressive strength of the modified sample was lower than that of the baseline sample. This may be due to the presence of ethylene glycol and nitric acid in the BiOBr precursor solution, not favoring the hydration of the cement upon addition.

4.2. Durability

For the materials prepared using the external admixture method, more consideration should be given to the wear resistance of the photocatalytic material as a coating [84,85], directly affecting the photocatalytic efficiency. Hassan et al. [71] prepared 10 mm thick concrete photocatalytic materials on the roads. These materials were tested for 20,000 road cycles. The results showed that the rutting depth of pure cement and two sets of composites containing different contents of photoactive material varied with the number of wheel cycles (Fig. 8). Results indicate that the application of the coating does not affect the wear resistance of the surface. Therefore, all three types of specimens are qualified for wear resistance.

Feng et al. [81] carried out more comprehensive cement durability tests on the photocatalytic cement for evaluating the penetration resistance, chloride ion corrosion, and carbonation. The composites exhibited superior resistance to penetration and chloride ion corrosion due to the catalytic waterproofing layer compared to pure cement. $Ca(OH)_2$ in

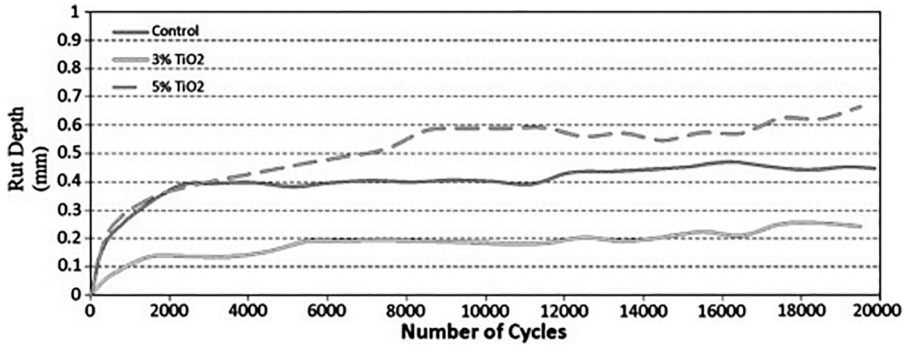

Fig. 8. Measured rut depth in the loaded wheel tester [71].

the cement mortar reacts with CO_2 in the air and carbonizes, reducing the mechanical strength of the mortar. The catalyst coating on the surface minimizes the direct contact between the interior cement and air or contaminated air, endowing photocatalytic cements higher carbonation resistance than pure cement with extended service life. Lu et al. [64] evaluated the durability of the catalyst coated on the composite surface under extreme environments by placing the composite in deionized water to simulate a natural rainy-day environment using both mild agitations and vigorous ultrasonic shaking. The results showed that approximately 30% catalyst was removed from the surface after 10 cycles in the mild agitation experiment. However, only about 6% TiO_2 was further lost within 10–30 cycles. In contrast, approximately 44% catalyst was removed after 10 min of sonication. In both cases, the interior of the catalyst coating showed stronger adhesion, and weaker (external) adhesion was destroyed at higher loads (further away from the binding interface) [86].

4.3. Photocatalytic performance

4.3.1. Internal mixing method

He et al. [62] conducted NO photocatalytic degradation on concrete using a self-designed test apparatus that was validated with a blank control, recording changes in NO concentration. In addition, comparative experiments using different catalysts were carried out. Despite the use of different catalysts, all the cement materials achieved significant NO degradation within the specified time. Similarly, Janus et al. [63] carried out comparative experiments using pure cement samples and composite cements containing different weight percentages of catalyst for NO degradation under UV light irradiation (Fig. 9). As shown, for the photocatalytic cement the efficiency for NO degradation increased with the catalyst amount, reaching the best result by 5 wt% TiO_2. Chen et al. [61] used ordinary silicate cement and white cement as carriers to fix both rutile and anatase phases of TiO_2 photocatalysts. The contrast experiment showed that both TiO_2 phases could effectively degrade NO, even if the different crystalline phases showed with different degradation effects. The higher efficiency of the white cement-based composites can be related to the presence of metal elements in their composition, providing favorable conditions for electron migration of the catalyst. Concerning white cement, Singh et al. [18] conducted rhodamine B dye degradation in water by a white cement composite with nano-silver photocatalyst with needle morphology. A maximum degradation efficiency of 80% was achieved by increasing ZnO addition (0, 5, 10, 15 wt %).

Lu et al. [64] prepared a TiO_2-loaded foam cement for the degradation of methyl blue in water by adding a foaming agent, a traditional TiO_2-modified cement was used as a control group, demonstrating that the foam cement composite exhibited a greater degradation capacity thanks to a larger specific surface area. Geng et al. [65] demonstrated the photocatalytic degradation of both rhodamine B and NO using cement loaded with BiOBr at different high temperature curing times,

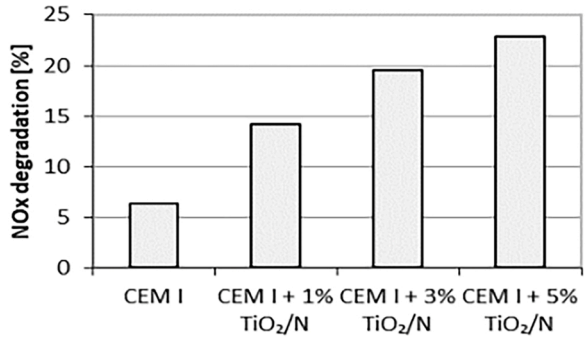

Fig. 9. Dependence of NO_x degradation [%] with the percentage of TiO_2/N added to cement by Janus et al. [63].

showing that the photocatalytic cements with longer curing times had higher efficiency towards both rhodamine B dye and NO (Fig. 10A and B). This result can be related to the increase in crystallinity of the photocatalyst with the temperature treatment.

4.3.2. Coating

Lu et al. [64] set up catalytic degradation experiments of NO in continuous by photocatalytic materials observing a decrease in NO content in ambient air after 2 h of UV irradiation. Loh et al. [87] investigated the ability of two coatings of ZnO and TiO_2 on the surface of cement blocks towards the abatement of bacteria and methylene blue (MB) under solar light irradiation, observing interesting results. Jafari et al. [88] immobilized TiO_2 and silica nanocomposite on white cement blocks by an immersion process for the photocatalytic degradation of dyes under UV light irradiation, showing higher degradation efficiency compared to the results obtained by nanocatalysts directly exposed to the dye. The enhanced effect can be related to the present of various cations in the cement composition, as confirmed by EDX analyses. Cement coated with BiOBr@SiO_2 achieved 74% degradation of rhodamine B dye and reduction of propylene concentration from 1000 ppm to 815 ppm within 2 h [73]. Peng et al. [76] used mica flakes and SnO_2 and g-C_3N_4 as photocatalysts to prepare photocatalytic cements for effectively degrading dyes as well as isopropanol, demonstrating that mica flakes worked as a barrier layer to prevent accelerated carbonization of cement from photocatalytic products, and SnO_2 acted as an electron transfer layer to accelerate the transfer of photogenerated electron pairs to the surface to participate in the degradation of pollutants. The prepared materials showed excellent photocatalytic performance after five cycles due to the creative catalyst that maximized photocatalytic activity and effectively protected the catalyst.

5. Applications

Japan was the first Country to study photocatalytic technology and to start photocatalytic technology industrialization work. According to a report in 1999 by China's Xinhua News Agency in Tokyo, Japan's Dongtao Company first fix photocatalytic films on the surface of tiles in 1998. This resulting product with antibacterial functions was the first building material product with photocatalytic capability for practical application. Today, several companies in Japan manufacture photocatalytic material-related products and are involved in photocatalytic-related technology development. For example, Kobe Steel has successfully developed photocatalytic iron decorative materials with antibacterial and anti-mold functions by using titanium metal as a cathode in the "AIP method" and discharging it in an oxygen environment to treat the surface of iron, thereby introducing a TiO_2 film on the surface of iron and applying it to the building decoration of medical and health institution buildings [89]. Japan Fujita has developed cement with the air-purifying ability and successfully laid this cementing material containing photocatalyst on the road to catalyze the degradation of automobile exhaust pollutants.

Photocatalytic materials are also widely used in civil engineering in many other Countries in United States and Europe. As for road tunnels, it is worth mentioning the Leopold II tunnel (Brussels) field campaign [90,91] in the framework of the European Life + PhotoPaq project, the "Umberto I" road tunnel in the city center of Rome [92], and smart roads in some European cities [86,93]. One of the first applications of photoactive building material in Europe is dated back to 2003 for the building of Jubilee Church in Rome (also known as *"Chiesa di Dio Padre Misericordioso"*) [86]. millennium TX®, a TiO_2-based active concrete by Italcementi was employed as the main building material. The presence of TiO_2 should have ensured self-cleaning properties and maintenance of the characteristic brilliant white color. Cardellicchio [86] monitored the state of Church walls 16 years after its building and noticed premature evidence of decay, indicating failure of the self-cleaning and color-preserving properties of its exposed precast concrete. He

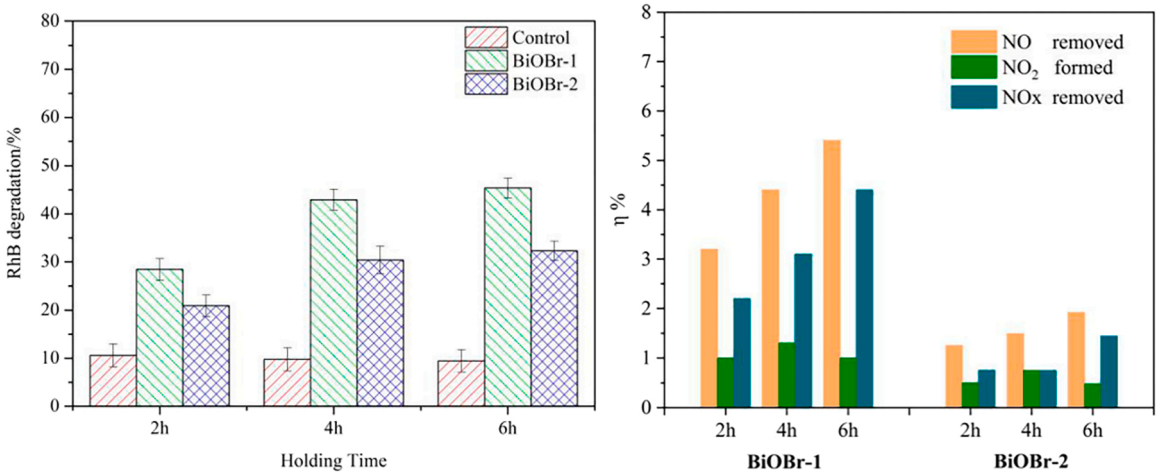

Fig. 10. Geng et al. [65]: (a) Percentage of RHB degradation rates on cement modified by BiOBr at different steam curing times and (b) NO-NO_x removal and NO_2 generation efficiency by the same materials.

attributed the loss of effectiveness to a synergistic effect between inorganic pollutants accumulation that cannot be oxidized by titania, and convex walls that do not allow rainwater runoff with subsequent water accumulation and erosion of the photoactive surface. Similar results were observed in ref II road tunnel case study investigated by Boonen et al. [90] and Gallus et al. [91] during a field campaign in this high-traffic road tunnel in Brussels (Belgium) before and after the coating of the internal wall and ceiling of a 160-meter length section, over a total tunnel length of more than 3 km, with TX Active® TiO_2--based coating from Italcementi, to obtain 2700 m^2 of photoactive surface, using a Supratec HTC 241 R7s light bulbs from Osram as the UV radiation source. The concentration of NO, NO_2, and NO_x was monitored in three different situations: before and after photoactive coating, upwind and downwind, and with UV lamp on and off. In all three cases, no statistically significant photocatalytic activity in terms of NO_x reduction was observed. The authors ascribed the poor results to low UV irradiance (1.6 $W{\cdot}m^{-2}$ against 4 $W{\cdot}m^{-2}$ necessary for optimal functioning of the photoactive cement) and high humidity combined with a premature decay of photocatalytic properties due to the fouling of active surfaces. In fact, the accumulation of dust in 3 km road tunnel can be faster than the photodegradation rate and the absence of rainfall cannot wash up the tunnel wall. All these factors can easily lead to the passivation of active surfaces, reducing their remediation properties. On the contrary, Guerrini [92] demonstrated a decrease in NO_x level statistically comparing NO_x pollution before and after the renewal of the "Umberto I" tunnel, a high traffic road in the city center of Rome, with the same TiO_2-based commercial coating used in Leopold II, the TX Active® from Italcementi. In this case, the wall was painted for the entire length of the tunnel, around 348 m, to obtain a photoactive area of around 9000 m^2 in contrast to the Leopold II tunnel case study, where only a small section was treated with the active material. In addition, the lighting system was upgraded by means of lamps with emission in the UV-A region, although no further specifications were given by the author. A 2–3-weeks field campaign was carried out in July (before renovation) and between September and October 2007 (after renovation) measuring the NO_x/CO_2 ratio in three zones: in the center of the tunnel, at the entrance, and at the exit. The importance of monitoring the NO_x/CO_2 ratio is due to the fact that NO_x and CO_2 are emitted by the same sources (e.g., vehicular traffic), but only NO_x is removed by titania. Data collected by two meteorological stations placed away from the tunnel but near roads with comparable traffic loads were used as background. The author recorded a decrease in NO_x level inside the tunnel by 21% before the renovation of the internal wall. Considering that background levels of NO_x in Rome were 61% during the second campaign period (July-September), the adjusted value of NO_x abatement is calculated to be between 51% and 64%. Investigating the variance of NO_x level, the author also noticed a reduction of NO_x peaks after renovation. If compared with the results obtained by Boonen et al. for the Leopold II tunnel, the degradation of the active surface over a short time was lower. However, some pictures taken 11 years after painting by Serpone [94] showed a certain wear of coating, probably due to dirt, dust, and NO_3^-, an accumulation that cannot be naturally washed off in a closed environment like a road tunnel. As observed by Yang et al. [60], for this type of indoor application, careful and regular maintenance is necessary to ensure the removal of the accumulated material, like inorganic dust and dirt, from the surface and UV lamp to maintain photocatalytic properties and UV irradiation at optimal levels. Ballari and coworkers [93] carried out a comparative study between a smart road, treated with a TiO_2--based coating, and a traditional road in Hengelo (the Netherlands) between January 2008 and July 2011. The coating of the smart road was realized by spraying 4 wt% suspension of carbon doped TiO_2 Kronos over 750 m^2 paving, obtaining an active surface with 2.7 g/m^2 of TiO_2. Field measurements showed a decrease of 19.2% in NO_x concentrations, considering the whole day average, and 28.3% considering only the afternoon average: the higher efficiency of the smart road in the afternoon hours can be attributed to a higher average solar irradiance and less humidity. However, a decreasing in efficiency was observed during the summer days and drought periods, probably due to nitrates and dust accumulation on the road surface. In fact, as already observed in other studies, photocatalytic surfaces easily lose their effectiveness, if not properly cleaned and maintained. The authors also noticed that after one year since laying the active surface loses its photocatalytic properties, as expected in a highly stressful environment, like an urban road. A similar result was obtained by Folli and co-workers [95] in a field campaign carried out in Copenhagen. A test-area of 100 m in Gasværksvej, a Copenhagen central street, was covered with TiO_2 containing concrete block provided by Starka Betongindustrier and followed by 100 m of control-area with standard concrete block. Two EcoPhysics CLD 66 chemiluminescence detector was used to monitor NO, NO_2, and NO_x concentration with sampling probe placed 2 m above ground level. A meteorological station recorded temperature, relative humidity and also sunlight irradiance. After one year of data recording, the field campaign showed that NO level was 22% lower in the road section with photoactive surface. Other studies regarding the effectiveness of smart roads were conducted in Fulda (Hesse, Germany) [96], in Bergamo (Italy), in Vanves (France) and in Antwerp (Belgium). In the German city of Petersbergerstraße, an 800-meter-long section of sidewalk was renewed using a TiO_2-based paving block, obtaining a 4500 m^2 photoactive area, whereas the entire road surface was around 15,000 m^2. The street had a heavy traffic load of 24000–30000 vehicles *per* day, mostly cars and

motorcycles. NO_x measurements were taken at 10 cm (point #1) and 3 m (point #2) from the ground in two sampling points placed in opposite points on the street in the middle of treated zone. Same measurements were carried out in a reference section located beyond the smart street. The results showed a decrease in NO_x concentrations, compared to the reference section, of about 17% at 10 cm from the ground and 9% at 3 m from the ground in the sampling point #1 and between 3.5% (at 10 cm) and 0% (at 3 m) in sampling point #2. The great variability of the data obtained leads to doubts about the real effectiveness of the new paving and further investigations are necessary to interpret the results. The Borgo Palazzo Street case study was carried out by Italcementi covering 7000 m^2 of the first half section, ca. 500 m, of a two-way road in Bergamo with TX Active concrete paving blocks and the second one with standard asphalt. The NO_x concentration was measured at 30 cm and at 180 cm from ground level in both sections, photoactive and reference, for over two years. The results of long-term monitoring showed that in the photoactive section of the road the concentration of NO_x was 20% lower than that in the reference section if measured at 180 cm above ground level, whereas the NO_x reduction increased up to 30% considering measurement at 30 cm. A laboratory test showed that the used blocks, removed from the street after 18 months of service, that converted 34.1% of NO_x, after washing, can still degrade 40.1% NO_x. This last result is very exciting, if compared to 41% new blocks. Other studies focused attention on the behavior of TiO_2-cement panels and paints as walls of canyon streets, these kinds of urban street are characterized by air flows different from a normal road and more similar to a road tunnel. Moreover, the great variability of meteorological parameters makes more difficult an accurate quantification of NO_x levels [97]. Maggos et al. [98] carried out a field test with a pilot scale site built in Guerville (France): three artificial canyon streets at the scale 1:5 were built using containers as sidewall. The wall of the first canyon was left as a bare container wall and was used to measure meteorological data, such as wind speed, wind direction, relative humidity and temperature, inside canyons. The second one was coated with TiO_2 based concrete by Italcementi, and the third one coated with standard white cement and used as reference. A closed end perforated pipe was used to homogeneously distribute pollutants, coming from an engine exhaust connected to a distribution pipe. During the tests the concentrations of NO_x, VOCs, CO, CO_2, and SO_2 were measured together with meteorological parameters mentioned above. The collected data showed that the pollution was from 36.7% to 82.0% lower in photoactive coated canyon street than in reference street. The authors correlated these differences in abatement capacities to wind direction and speed that can reduce the residence time of pollutants near the photoactive surface. The dilution role of wind was already mentioned in the studies conducted in road tunnels, in some ways similar to canyon street, where vehicular traffic causes an artificial air current. Rue Jean Bleuzen is another canyon street in Vanves, France. During its redevelopment the pavement and sidewalks were rebuilt using TX Active cement by Italcementi. The Italian company then conducted an air quality study confirming an average 20% reduction in NO_x concentrations compared to pre-renovation levels. Tremper and Green [99] drafted a technical report in 2016 about walls painting with 120–150 $g{\cdot}m^{-2}$ of a specific photoactive TiO_2 based coating of Artwork Elephant area, a creative hub in central London. The data were collected by in-site monitoring station before and after repainting. The background level was collected by four monitoring sites within the inner ring road and used as control sites. Statistical analysis found a negligible decreasing of NO_x pollution level and authors ascribed the poor results to seasonal meteorological variation and traffic volume changes during the data collection period. A similar result had been obtained some year before, in 2011, by The Netherlands' Directorate-General for Public Works and Water Management in the framework of the Dutch Air Quality Innovation Programme. As part of the program, a study [100] was carried out replacing standard concrete barrier with TiO_2 concrete barrier and a special porous TiO_2--concrete barrier respectively on A1 near Treschun and A28 near Putten. No evidence of an improvement of air quality (measured as NO_x levels) was found, poor results was ascribed to high variability of external condition such as traffic volume, humidity and contact time between air and active surface. Kim et al. [101] carried out a study based on the treatment of the concrete surface of retaining wall of Gyeongbu expressway in Korea by a mixture of TiO_2 and penetrating agent. The active material loading was calculated to be around 500 g/m^2. Measurements were taken above the surface of a treated section of 150 × 1.9 m and compared to those taken above surface of a control section of 200 × 1.9 m. The results of data collection during the field campaign showed a decreasing of 13% NO_x level after treatment. As already noticed by other authors sunlight irradiance, meteorological conditions and traffic load were a key variable that affect results of monitoring.

The research of photocatalytic materials in China started late, but with the urgent need for practical necessities and strong support of national policies, its research progress and application have shown strong momentum and broad prospects. In terms of application, in 2001, according to Beijing Daily, a Chinese company used nanocoatings with photocatalytic effect to decorate three stadiums, including Beijing Capital Stadium, Beijing Workers Stadium, and Beijing Olympic Sports Center, as well as many district buildings in Beijing. The initiative had good effects on the appearance of buildings to maintain long-term cleanliness. Qian et al. [102] sprayed a nano-TiO_2 photocatalytic water agent on the pavement near the square of the toll station north of the Nanjing Yangtze River Third Bridge under construction and tested and positively evaluated the catalytic effect of the concrete pavement on the NO_x emission in automobile exhaust after the official opening to traffic. In March 2013, in Kunming City, Yunnan Province, Yunling Transportation Technology Company, and Shenzhen Haichuan Ltd. responded to the national call through joint research to develop a green photocatalytic coating based on a project on car exhaust absorption near a highway toll station in Kunming, exploiting the photocatalytic properties of the coating, so that the lanes on both sides of the toll station adsorb and degrade the harmful substances in car exhaust, and improve the air quality near the toll station. Meng et al. [103] conducted a field test on nano-TiO_2 photocatalytic concrete to purify the air from nitrogen oxides in the toll station section near the national highway Jingga Highway (G111 line), and the results showed that the test section had a good photocatalytic degradation effect.

6. Summary and outlook

This review critically summarizes the state-of-the-art of cementitious materials loaded with photocatalysts as a new type of composite with great potential for applications, able not only to enhance the physical properties of the cementitious material itself but also to give it the ability to degrade pollutants. As a basic building product, cement-based photocatalytic materials need to have reliable mechanical properties on the one hand, and consistent efficiency in degrading pollutants on the other hand.

In the present review different approaches for the fabrication of photocatalytic cements were accurately reported and critically faced, highlighting the strengths and weaknesses of each method.

Moreover, the effect of particles load on the mechanical features of concretes has been evaluated on the basis of the data reported in the scientific literature. The results permit to conclude that compressive and flexural strength, modulus of elasticity, chloride corrosion resistance, carbonation and many other mechanical aspects are affected by the amount of particles introduced in the cement. Depending on the preparation method used, the optimization of the load must be suitably evaluated, since an excess of particles leads to a deterioration of the mechanical performances. The photodegradation abilities of photoactive concretes towards NOx, as well as dyes and other pollutants, have been properly investigated. If on the one hand the photodegradation tests carried out in lab scale are mostly always promising, on the other

hand for real applications is not possible to reach definitive conclusions. In general, the poor and often conflicting results can be attributed to the different meteorological conditions present at the time of the tests (wind speed, humidity level, irradiation level, rainfall level, etc.), as well as the traffic intensity too variable, which strongly affect the performance of the materials. Therefore, although the most part of the developed photoactive cements are promising to fight air pollution, for real application some precautions and suitable maintenance procedures are necessary to avoid particles' detachment and their deactivation due to the accumulation of dust and dirt on the surface.

Declaration of Competing Interest

The authors declare that they have no known competing financial interests or personal relationships that could have appeared to influence the work reported in this paper.

Data Availability

No data was used for the research described in the article.

Acknowledgments

This work is financially supported by the Key Research and Development Program of Ningbo (2022Z178), China Construction Technology Research and Development Project (CSCEC-2021-Z-5–02), CSCEC Western Construction Science and Technology Plan (ZJXJ-2021–03), Fundamental Research Funds for the Provincial Universities of Zhejiang (2020YW53), and the Department of Education of Zhejiang Province (Y202249428).

References

[1] X. Ma, Emergent Social Complexity in the Yangshao Culture: Analyses of settlement patterns and faunal remains from Lingbau Western Henan China (c. 4900-3000 BC), BAR Publishing, 2005.
[2] G. Bastos, F. Patiño-Barbeito, F. Patiño-Cambeiro, J. Armesto, Admixtures in cement-matrix composites for mechanical reinforcement, sustainability, and smart features, Materials 9 (12) (2016) 972, https://doi.org/10.3390/ma9120972.
[3] H.G. Van Oss, A.C. Padovani, Cement manufacture and the environment: part I: chemistry and technology, J. Ind. Ecol. 6 (1) (2002) 89–105, https://doi.org/10.1162/108819802320971650.
[4] G. Kheder, A. Al Gabban, S. Abid, Mathematical model for the prediction of cement compressive strength at the ages of 7 and 28 days within 24 h, Mater. Struct. 36 (10) (2003) 693–701, https://doi.org/10.1007/BF02479504.
[5] M. Schneider, M. Romer, M. Tschudin, H. Bolio, Sustainable cement production—present and future, Cem. Concr. Res. 41 (7) (2011) 642–650, https://doi.org/10.1016/j.cemconres.2011.03.019.
[6] C.L. Sabine, R.A. Feely, N. Gruber, R.M. Key, K. Lee, J.L. Bullister, R. Wanninkhof, C. Wong, D.W. Wallace, B. Tilbrook, The oceanic sink for anthropogenic CO_2, Science 305 (5682) (2004) 367–371, https://doi.org/10.1126/science.1097403.
[7] R.A. Feely, C.L. Sabine, K. Lee, W. Berelson, J. Kleypas, V.J. Fabry, F.J. Millero, Impact of anthropogenic CO_2 on the $CaCO_3$ system in the oceans, Science 305 (5682) (2004) 362–366, https://doi.org/10.1126/science.1097329.
[8] M. Ali, R. Saidur, M. Hossain, A review on emission analysis in cement industries, Renew. Sustain. Energy Rev. 15 (5) (2011) 2252–2261, https://doi.org/10.1016/j.rser.2011.02.014.
[9] U. Kääntee, R. Zevenhoven, R. Backman, M. Hupa, Cement manufacturing using alternative fuels and the advantages of process modelling, Fuel Process. Technol. 85 (4) (2004) 293–301, https://doi.org/10.1016/S0378-3820(03)00203-0.
[10] A.A. Usón, A.M. López-Sabirón, G. Ferreira, E.L. Sastresa, Uses of alternative fuels and raw materials in the cement industry as sustainable waste management options, Renew. Sustain. Energy Rev. 23 (2013) 242–260, https://doi.org/10.1016/j.rser.2013.02.024.
[11] L. Vizcaíno-Andrés, S. Sánchez-Berriel, S. Damas-Carrera, A. Pérez-Hernández, K. Scrivener, J. Martirena-Hernández, Industrial trial to produce a low clinker, low carbon cement, e045-e045, Mater. De. Constr. 65 (317) (2015), https://doi.org/10.3989/mc.2015.00614.
[12] E. Gartner, T. Sui, Alternative cement clinkers, Cem. Concr. Res. 114 (2018) 27–39, https://doi.org/10.1016/j.cemconres.2017.02.002.
[13] Z. Liu, W. Hansen, Effect of hydrophobic surface treatment on freeze-thaw durability of concrete, Cem. Concr. Compos. 69 (2016) 49–60, https://doi.org/10.1016/j.cemconcomp.2016.03.001.
[14] P. Steffan, P. Barath, J. Stehlik, R. Vrba, The multifunction conducting materials base on cement concrete with carbon fibers, Electronics (2008).
[15] H. Tong, S. Ouyang, Y. Bi, N. Umezawa, M. Oshikiri, J. Ye, Nano-photocatalytic materials: possibilities and challenges, Adv. Mater. 24 (2) (2012) 229–251, https://doi.org/10.1002/adma.201102752.
[16] M.C.P. Menor, P.S. Ros, A.M. García, M.J.A. Caballero, Granulated cork with bark characterised as environment-friendly lightweight aggregate for cement based materials, J. Clean. Prod. 229 (2019) 358–373, https://doi.org/10.1016/j.jclepro.2019.04.154.
[17] A.H. Mahmoudkhani, D. Huynh, C.J. Sylvestre, J. Schneider In New environment-friendly cement slurries with enhanced mechanical properties for gas well cementing, CIPC/SPE Gas Technology Symposium 2008 Joint Conference, OnePetro: 2008.
[18] V. Singh, K. Sandeep, H. Kushwaha, S. Powar, R. Vaish, Photocatalytic, hydrophobic and antimicrobial characteristics of ZnO nano needle embedded cement composites, Constr. Build. Mater. 158 (2018) 285–294, https://doi.org/10.1016/j.conbuildmat.2017.10.035.
[19] D.G. Fullerton, N. Bruce, S.B. Gordon, Indoor air pollution from biomass fuel smoke is a major health concern in the developing world, Trans. R. Soc. Trop. Med. Hyg. 102 (9) (2008) 843–851, https://doi.org/10.1016/j.trstmh.2008.05.028.
[20] O.P. Kurmi, S. Semple, P. Simkhada, W.C.S. Smith, J.G. Ayres, COPD and chronic bronchitis risk of indoor air pollution from solid fuel: a systematic review and meta-analysis, Thorax 65 (3) (2010) 221–228.
[21] Y. Zhang, J. Mo, Y. Li, J. Sundell, P. Wargocki, J. Zhang, J.C. Little, R. Corsi, Q. Deng, M.H. Leung, Can commonly-used fan-driven air cleaning technologies improve indoor air quality? A literature review, Atmos. Environ. 45 (26) (2011) 4329–4343, https://doi.org/10.1016/j.atmosenv.2011.05.041.
[22] M. Schiavello, Photoelectrochemistry, Photocatalysis and Photoreactors Fundamentals and Developments Vol. 146, Springer Science & Business Media, 2013.
[23] A. Mills, S.Le Hunte, An overview of semiconductor photocatalysis, J. Photochem. Photobiol. A: Chem. 108 (1) (1997) 1–35, https://doi.org/10.1016/S1010-6030(97)00118-4.
[24] H. Ren, P. Koshy, W.F. Chen, S. Qi, C.C. Sorrell, Photocatalytic materials and technologies for air purification, J. Hazard. Mater. 325 (2017) 340–366, https://doi.org/10.1016/j.jhazmat.2016.08.072.
[25] K. Maeda, K. Domen, New non-oxide photocatalysts designed for overall water splitting under visible light, J. Phys. Chem. C. 111 (22) (2007) 7851–7861, https://doi.org/10.1021/jp070911w.
[26] X. Wang, K. Maeda, A. Thomas, K. Takanabe, G. Xin, J.M. Carlsson, K. Domen, M. Antonietti, A metal-free polymeric photocatalyst for hydrogen production from water under visible light, Nat. Mater. 8 (1) (2009) 76–80, https://doi.org/10.1038/nmat2317.
[27] L. Jing, W.J. Ong, R. Zhang, E. Pickwell-MacPherson, C.Y. Jimmy, Graphitic carbon nitride nanosheet wrapped mesoporous titanium dioxide for enhanced photoelectrocatalytic water splitting, Catal. Today 315 (2018) 103–109, https://doi.org/10.1016/j.cattod.2018.04.007.
[28] Y. Kang, Y. Yang, L.C. Yin, X. Kang, G. Liu, H.M. Cheng, An amorphous carbon nitride photocatalyst with greatly extended visible-light-responsive range for photocatalytic hydrogen generation, Adv. Mater. 27 (31) (2015) 4572–4577, https://doi.org/10.1002/adma.201501939.
[29] M.Z. Rahman, K. Davey, C.B. Mullins, Tuning the intrinsic properties of carbon nitride for high quantum yield photocatalytic hydrogen production, Adv. Sci. 5 (10) (2018) 1800820, https://doi.org/10.1002/advs.201800820.
[30] A. Yadav, S.W. Kang, Y. Hunge, Photocatalytic degradation of Rhodamine B using graphitic carbon nitride photocatalyst, J. Mater. Sci.: Mater. Electron. 32 (11) (2021) 15577–15585, https://doi.org/10.1007/s10854-021-06106-y.
[31] L. Ma, G. Wang, C. Jiang, H. Bao, Q. Xu, Synthesis of core-shell TiO_2@ g-C_3N_4 hollow microspheres for efficient photocatalytic degradation of rhodamine B under visible light, Appl. Surf. Sci. 430 (2018) 263–272, https://doi.org/10.1016/j.apsusc.2017.07.282.
[32] H. Zhao, H. Yu, X. Quan, S. Chen, Y. Zhang, H. Zhao, H. Wang, Fabrication of atomic single layer graphitic-C_3N_4 and its high performance of photocatalytic disinfection under visible light irradiation, Appl. Catal. B: Environ. 152 (2014) 46–50, https://doi.org/10.1016/j.apcatb.2014.01.023.
[33] X. Wang, W. Xiong, X. Li, Q. Zhao, S. Fan, M. Zhang, J. Mu, A. Chen, Fabrication of MoS_2@ g-C_3N_4 core-shell nanospheres for visible light photocatalytic degradation of toluene, J. Nanopart. Res. 20 (9) (2018) 1–12, https://doi.org/10.1007/s11051-018-4340-1.
[34] D. Lu, H. Wang, X. Zhao, K.K. Kondamareddy, J. Ding, C. Li, P. Fang, Highly efficient visible-light-induced photoactivity of Z-scheme g-C_3N_4/Ag/MoS_2 ternary photocatalysts for organic pollutant degradation and production of hydrogen, ACS Sustain. Chem. Eng. 5 (2) (2017) 1436–1445, https://doi.org/10.1021/acssuschemeng.6b02010.
[35] B. Tatykayev, B. Chouchene, L. Balan, T. Gries, G. Medjahdi, B. Uralbekov, R. Schneider, Heterostructured g-CN/TiO_2 photocatalysts prepared by thermolysis of g-CN/MIL-125(Ti) composites for efficient pollutant degradation and hydrogen production, Nanomaterials 10 (7) (2020) 1387, https://doi.org/10.3390/nano10071387.
[36] A. Kumar, G. Sharma, A. Kumari, C. Guo, Mu Naushad, D.V.N. Vo, J. Iqbal, F. J. Stadler, Construction of dual Z-scheme g-C_3N_4/$Bi_4Ti_3O_{12}$/$Bi_4O_5I_2$ heterojunction for visible and solar powered coupled photocatalytic antibiotic degradation and hydrogen production: boosting via I^-/I_3^- and Bi^{3+}/Bi^{5+} redox mediators, Appl. Catal. B: Environ. 284 (2021), 119808, https://doi.org/10.1016/j.apcatb.2020.119808.
[37] A. Kudo, Y. Miseki, Heterogeneous photocatalyst materials for water splitting, Chem. Soc. Rev. 38 (1) (2009) 253–278, https://doi.org/10.1039/B800489G.

[38] N.C. Zheng, T. Ouyang, Y. Chen, Z. Wang, D.Y. Chen, Z.Q. Liu, Ultrathin CdS shell-sensitized hollow S-doped CeO_2 spheres for efficient visible-light photocatalysis, Catal. Sci. Technol. 9 (6) (2019) 1357–1364, https://doi.org/10.1039/C8CY02206B.

[39] Y. Xu, M.A. Schoonen, The absolute energy positions of conduction and valence bands of selected semiconducting minerals, Am. Mineral. 85 (3–4) (2000) 543–556, https://doi.org/10.2138/am-2000-0416.

[40] L. Wei, Z. Guo, X. Jia, Probing photocorrosion mechanism of CdS films and enhancing photoelectrocatalytic activity via cocatalyst, Catal. Lett. 151 (1) (2021) 56–66, https://doi.org/10.1007/s10562-020-03275-z.

[41] X. Ning, G. Lu, Photocorrosion inhibition of CdS-based catalysts for photocatalytic overall water splitting, Nanoscale 12 (3) (2020) 1213–1223, https://doi.org/10.1039/C9NR09183A.

[42] A. Fujishima, K. Honda, Electrochemical photolysis of water at a semiconductor electrode, Nature 238 (5358) (1972) 37–38, https://doi.org/10.1038/238037a0.

[43] M.G. Galloni, G. Cerrato, A. Giordana, E. Falletta, C.L. Bianchi, Sustainable solar light photodegradation of diclofenac by nano- and micro-sized SrTiO3, Catalysts 12 (8) (2022) 804, https://doi.org/10.3390/catal12080804.

[44] H. Zhou, Y. Qu, T. Zeid, X. Duan, Towards highly efficient photocatalysts using semiconductor nanoarchitectures, Energy Environ. Sci. 5 (5) (2012) 6732–6743, https://doi.org/10.1039/C2EE03447F.

[45] S.Y. Chai, Y.J. Kim, M.H. Jung, A.K. Chakraborty, D. Jung, W.I. Lee, Heterojunctioned $BiOCl/Bi_2O_3$, a new visible light photocatalyst, J. Catal. 262 (1) (2009) 144–149, https://doi.org/10.1016/j.jcat.2008.12.020.

[46] L. Zhang, W. Wang, J. Yang, Z. Chen, W. Zhang, L. Zhou, S. Liu, Sonochemical synthesis of nanocrystallite Bi_2O_3 as a visible-light-driven photocatalyst, Appl. Catal. A: Gen. 308 (2006) 105–110, https://doi.org/10.1016/j.apcata.2006.04.016.

[47] M.G. Galloni, E. Ferrara, E. Falletta, C.L. Bianchi, Olive mill wastewater remediation: from conventional approaches to photocatalytic processes by easily recoverable materials, Catalysts 12 (8) (2022) 923, https://doi.org/10.3390/catal12080923.

[48] A. Cabot, A. Marsal, J. Arbiol, J. Morante, Bi_2O_3 as a selective sensing material for NO detection, Sens. Actuators B: Chem. 99 (1) (2004) 74–89, https://doi.org/10.1016/j.snb.2003.10.032.

[49] N. Sammes, G. Tompsett, H. Näfe, F. Aldinger, Bismuth based oxide electrolytes—structure and ionic conductivity, J. Eur. Ceram. Soc. 19 (10) (1999) 1801–1826, https://doi.org/10.1016/S0955-2219(99)00009-6.

[50] X. Meng, Z. Zhang, Bismuth-based photocatalytic semiconductors: introduction, challenges and possible approaches, J. Mol. Catal. A: Chem. 423 (2016) 533–549, https://doi.org/10.1016/j.molcata.2016.07.030.

[51] Y. Xie, Y. Zhou, C. Gao, L. Liu, Y. Zhang, Y. Chen, Y. Shao, Construction of AgBr/BiOBr S-scheme heterojunction using ion exchange strategy for high-efficiency reduction of CO_2 to CO under visible light, Sep. Purif. Technol. 303 (2022), 122288, https://doi.org/10.1016/j.seppur.2022.122288.

[52] Z. Miao, Q. Wang, Y. Zhang, L. Meng, X. Wang, In situ construction of S-scheme AgBr/BiOBr heterojunction with surface oxygen vacancy for boosting photocatalytic CO_2 reduction with H2O, Appl. Catal. B: Environ. 301 (2022), 120802, https://doi.org/10.1016/j.apcatb.2021.120802.

[53] J. Lyu, Z. Li, M. Ge, Novel Bi/BiOBr/AgBr composite microspheres: Ion exchange synthesis and photocatalytic performance, Solid State Sci. 80 (2018) 101–109, https://doi.org/10.1016/j.solidstatesciences.2018.04.004.

[54] S.-H. Liu, W.-X. Lin, A simple method to prepare g-C_3N_4-TiO_2/waste zeolites as visible-light-responsive photocatalytic coatings for degradation of indoor formaldehyde, J. Hazard. Mater. 368 (2019) 468–476, https://doi.org/10.1016/j.jhazmat.2019.01.082.

[55] S. Campisi, M.G. Galloni, S.G. Marchetti, A. Auroux, G. Postole, A. Gervasini, Functionalized Iron Hydroxyapatite as Eco-friendly Catalyst for NH_3-SCR Reaction: Activity and Role of Iron Speciation on the Surface, ChemCatChem 12 (2020) 1676–1690, https://doi.org/10.1002/cctc.201901813.

[56] M.G. Galloni, S. Campisi, S.G. Marchetti, A. Gervasini, Environmental reactions of air-quality protection on eco-friendly iron-based catalysts, Catalysts 10 (12) (2020) 1–19, https://doi.org/10.3390/catal10121415.

[57] S. Campisi, M.G. Galloni, F. Bossola, A. Gervasini, Comparative performance of copper and iron functionalized hydroxyapatite catalysts in NH_3-SCR, Catal. Commun. 123 (2019) 79–85, https://doi.org/10.1016/j.catcom.2019.02.008.

[58] H.S. Koren, Associations between criteria air pollutants and asthma, Environ. Health Perspect. 103 (suppl 6) (1995) 235–242, https://doi.org/10.1289/ehp.95103s6235.

[59] D. Seo, T.S. Yun, NOx removal rate of photocatalytic cementitious materials with TiO_2 in wet condition, Build. Environ. 112 (2017) 233–240, https://doi.org/10.1016/j.buildenv.2016.11.037.

[60] L. Yang, A. Hakki, F. Wang, D.E. Macphee, Photocatalyst efficiencies in concrete technology: the effect of photocatalyst placement, Appl. Catal. B: Environ. 222 (2018) 200–208, https://doi.org/10.1016/j.apcatb.2017.10.013.

[61] J. Chen, C.S. Poon, Photocatalytic cementitious materials: influence of the microstructure of cement paste on photocatalytic pollution degradation, Environ. Sci. Technol. 43 (23) (2009) 8948–8952, https://doi.org/10.1021/es902359s.

[62] R. He, X. Huang, J. Zhang, Y. Geng, H. Guo, Preparation and evaluation of exhaust-purifying cement concrete employing titanium dioxide, Materials 12 (13) (2019) 2182, https://doi.org/10.3390/ma12132182.

[63] M. Janus, S. Mądraszewski, K. Zając, E. Kusiak-Nejman, A.W. Morawski, D. Stephan, D, Photocatalytic activity and mechanical properties of cements modified with TiO_2/N, Materials 12 (22) (2019) 3756, https://doi.org/10.3390/ma12223756.

[64] Z. Lu, Q. Wang, R. Yin, B. Chen, Z. Li, A novel TiO_2/foam cement composite with enhanced photodegradation of methyl blue, Constr. Build. Mater. 129 (2016) 159–162, https://doi.org/10.1016/j.conbuildmat.2016.10.105.

[65] Z. Geng, L. Zhang, J. Wang, Y. Yu, G. Zhang, X. Cheng, D. Wang, BiOBr precursor solutions modified cement paste: the photocatalytic performance and effects, Crystals 11 (8) (2021) 969, https://doi.org/10.3390/cryst11080969.

[66] J. Hierrezuelo, A. Sadeghpour, I. Szilagyi, A. Vaccaro, M. Borkovec, Electrostatic stabilization of charged colloidal particles with adsorbed polyelectrolytes of opposite charge, Langmuir 26 (19) (2010) 15109–15111, https://doi.org/10.1021/la102912u.

[67] N. Mandzy, E. Grulke, T. Druffel, Breakage of TiO_2 agglomerates in electrostatically stabilized aqueous dispersions, Powder Technol. 160 (2) (2005) 121–126, https://doi.org/10.1016/j.powtec.2005.08.020.

[68] X. Zhang, Preparation of photocatalytic cement slurry and its degradation performance on automobile exhaust gas, Cent. South Univ. (2014).

[69] R. Djellabi, D. Aboagye, D, M.G. Galloni, V.V. Andhalkar, S. Nouacer, W. Nabgan, S. Rtimi, M. Constantí, F. Medina Cabello, S. Contreras, Combined conversion of lignocellulosic biomass into high-value products with ultrasonic cavitation and photocatalytic produced reactive oxygen species – a review, Bioresour. Technol. 368 (2023), 128333, https://doi.org/10.1016/j.biortech.2022.128333.

[70] E. Serelis, V. Vaitkevicius, H. Hilbig, L. Irbe, Z. Rudzionis, Effect of ultra-sonic dispersion time on hydration process and microstructure development of ultra-high performance glass powder concrete, Constr. Build. Mater. 298 (2021), 123856, https://doi.org/10.1016/j.conbuildmat.2021.123856.

[71] M.M. Hassan, H. Dylla, L.N. Mohammad, T. Rupnow, Evaluation of the durability of titanium dioxide photocatalyst coating for concrete pavement, Constr. Build. Mater. 24 (8) (2010) 1456–1461, https://doi.org/10.1016/j.conbuildmat.2010.01.009.

[72] S. Feng, J. Song, F. Liu, X. Fu, H. Guo, J. Zhu, Q. Zeng, X. Peng, X. Wang, Y. Ouyang, Photocatalytic properties, mechanical strength and durability of TiO_2/cement composites prepared by a spraying method for removal of organic pollutants, Chemosphere 254 (2020), 126813, https://doi.org/10.1016/j.chemosphere.2020.126813.

[73] D. Wang, P. Hou, P. Yang, X. Cheng, $BiOBr@SiO_2$ flower-like nanospheres chemically-bonded on cement-based materials for photocatalysis, Appl. Surf. Sci. 430 (2018) 539–548, https://doi.org/10.1016/j.apsusc.2017.07.202.

[74] R. Baan, K. Straif, Y. Grosse, B. Secretan, F. El Ghissassi, V. Cogliano, Carcinogenicity of carbon black, titanium dioxide, and talc, Lancet Oncol. 7 (4) (2006) 295–296.

[75] I. Guseva Canu, S. Fraize-Frontier, C. Michel, S. Charles, Weight of epidemiological evidence for titanium dioxide risk assessment: current state and further needs, J. Expo. Sci. Environ. Epidemiol. 30 (3) (2020) 430–435, https://doi.org/10.1038/s41370-019-0161-2.

[76] F. Peng, Y. Ni, Q. Zhou, J. Kou, C. Lu, Z. Xu, New g-C_3N_4 based photocatalytic cement with enhanced visible-light photocatalytic activity by constructing muscovite sheet/SnO_2 structures, Constr. Build. Mater. 179 (2018) 315–325, https://doi.org/10.1016/j.conbuildmat.2018.05.146.

[77] B.Y. Lee, K.E. Kurtis, Influence of TiO_2 nanoparticles on early C_3S hydration, J. Am. Ceram. Soc. 93 (10) (2010) 3399–3405, https://doi.org/10.1111/j.1551-2916.2010.03868.x.

[78] J.H. Chen, High-performance concrete application status and its prospect, Guangdong Civil Eng. Constr. 05 (2000) 3–8, https://doi.org/10.1061/~ASCE!0733-9364–2005!131:4–459.

[79] R. Zhang, X. Cheng, P. Hou, Z. Ye, Influences of nano-TiO_2 on the properties of cement-based materials: Hydration and drying shrinkage, Constr. Build. Mater. 81 (2015) 35–41, https://doi.org/10.1016/j.conbuildmat.2015.02.003.

[80] B.G. Ma, N.H. Li, J.P. Mei, L. Han, Toughening effect and mechanism of action of nano-TiO_2 on cement-based materials, J. Funct. Mater. 46 (12) (2015) 12065–12069.

[81] L.C. Feng, C.W. Gong, Y.P. Wu, D.C. Feng, N. Xie, In The study on mechanical properties and microstructure of cement paste with nano-TiO_2, Adv. Mater. Res. Trans. Tech. Publ. (2013) 477–481.

[82] P. Maravelaki-Kalaitzaki, Z. Agioutantis, E. Lionakis, M. Stavroulaki, V. Perdikatsis, Physico-chemical and mechanical characterization of hydraulic mortars containing nano-titania for restoration applications, Cem. Concr. Compos. 36 (2013) 33–41, https://doi.org/10.1016/j.cemconcomp.2012.07.002.

[83] C. Liang, Y.Q. Wu, D.W. Wang, H. Wang, Research progress of nano-TiO2 photocatalytic cement-based materials, Mater. Rep. 33 (S2) (2019) 267–272.

[84] E. Boonen, A. Beeldens, I. Dirkx, V. Bams, Durability of cementitious photocatalytic building materials, Catal. Today 287 (2017) 196–202, https://doi.org/10.1016/j.cattod.2016.10.012.

[85] A. Fiore, G.C. Marano, P. Monaco, A. Morbi, Preliminary experimental study on the effects of surface-applied photocatalytic products on the durability of reinforced concrete, Constr. Build. Mater. 48 (2013) 137–143, https://doi.org/10.1016/j.conbuildmat.2013.06.058.

[86] L. Cardellicchio, Self-cleaning and colour-preserving efficiency of photocatalytic concrete: case study of the Jubilee Church in Rome, Build. Res. Inf. 48 (2) (2020) 160–179, https://doi.org/10.1080/09613218.2019.1622405.

[87] K. Loh, C. Gaylarde, M. Shirakawa, Photocatalytic activity of ZnO and TiO_2 'nanoparticles' for use in cement mixes, Constr. Build. Mater. 167 (2018) 853–859, https://doi.org/10.1016/j.conbuildmat.2018.02.103.

[88] H. Jafari, S. Afshar, O. Zabihi, M. Naebe, M, Enhanced photocatalytic activities of TiO_2–SiO_2 nanohybrids immobilized on cement-based materials for dye degradation, Res. Chem. Intermed. 42 (4) (2016) 2963–2978, https://doi.org/10.1007/s11164-015-2190-3.

[89] M. Zhao, Monitoring and effectiveness evaluation of TiO_2 degradation of vehicle exhaust (NO_x) on asphalt pavement, Northeast For. Univ. (2013).
[90] E. Boonen, V. Akylas, F. Barmpas, A. Boréave, L. Bottalico, M. Cazaunau, H. Chen, V. Daële, T. De Marco, J. Doussin, Construction of a photocatalytic de-polluting field site in the Leopold II tunnel in Brussels, J. Environ. Manag. 155 (2015) 136–144, https://doi.org/10.1016/j.jenvman.2015.03.001.
[91] M. Gallus, V. Akylas, F. Barmpas, A. Beeldens, E. Boonen, A. Boréave, M. Cazaunau, H. Chen, H, V. Daële, J. Doussin, Photocatalytic de-pollution in the Leopold II tunnel in Brussels: NO_x abatement results, Build. Environ. 84 (2015) 125–133, https://doi.org/10.1016/j.buildenv.2014.10.032.
[92] G.L. Guerrini, Photocatalytic performances in a city tunnel in Rome: NO_x monitoring results, Constr. Build. Mater. 27 (1) (2012) 165–175, https://doi.org/10.1016/j.conbuildmat.2011.07.065.
[93] M.M. Ballari, H. Brouwers, Full scale demonstration of air-purifying pavement, J. Hazard. Mater. 254 (2013) 406–414, https://doi.org/10.1016/j.jhazmat.2013.02.012.
[94] N. Serpone, Heterogeneous photocatalysis and prospects of TiO_2-based photocatalytic DeNOxing the atmospheric environment, Catalysts 8 (11) (2018) 553, https://doi.org/10.3390/catal8110553.
[95] A. Folli, M. Strøm, T.P. Madsen, T. Henriksen, J. Lang, J. Emenius, T. Klevebrant, A. Nilsson, Field study of air purifying paving elements containing TiO_2, Atmos. Environ. 107 (2015) 44–51, https://doi.org/10.1016/j.atmosenv.2015.02.025.
[96] S. Jacobi, NO_2-Reduzierung Durch Photokatalytisch Wirksame Oberflächen, Modellversuch Fulda (Hesse, Germany) 2012.
[97] N. Moussiopoulos, P. Barmpas, I. Ossanlis, J. Bartzis, Comparison of numerical and experimental results for the evaluation of the depollution effectiveness of photocatalytic coverings in street canyons, Environ. Model. Assess. 13 (3) (2008) 357–368, https://doi.org/10.1007/s10666-007-9098-2.
[98] T. Maggos, A. Plassais, J. Bartzis, C. Vasilakos, N. Moussiopoulos, L. Bonafous, Photocatalytic degradation of Nox in a pilot street canyon configuration using TiO_2-mortar panels, Environ. Monit. Assess. 136 (1) (2008) 35–44, https://doi.org/10.1007/s10661-007-9722-2.
[99] A. Tremper, D. Green, Artworks D-NOX Paint Trial Report; Technical Report: 2016.
[100] I. Dutch, Innovation Programme concluded. 2010.
[101] Y.K. Kim, S.J. Hong, H.B. Kim, S.W. Lee, Evaluation of in-situ NOx removal efficiency of photocatalytic concrete in expressways, KSCE J. Civ. Eng. 22 (7) (2018) 2274–2280, https://doi.org/10.1007/s12205-017-0028-9.
[102] L. Li, C.X. Qian, Study on the removal of nitrogen oxides from automobile emissions by photocatalytic functional concrete road of Nanjing Yangtze River Third Bridge, J. Henan Univ. Sci. Technol. (Nat. Sci. Ed.) 30 (01) (2009) 49–52.
[103] Q. Guang, M. Chen, Study on spraying nano-TiO_2 on highway cement concrete pavement to purify pollutants emitted from motor vehicles, Road Traffic Technol. 26 (03) (2009) 154–158.